Investigations on the performance and the robustness of a metabsorber designed for structural vibration mitigation

Emmanuel Bachy, Kévin Jaboviste, Emeline Sadoulet-Reboul, Nicolas Peyret, Gaël Chevallier, Charles Arnould, Eric Collard

Investigations on the performance and the robustness of a metabsorber designed for structural vibration mitigation

Emmanuel Bachy[a], Kévin Jaboviste[a], Emeline Sadoulet-Reboul[a,], Nicolas Peyret[c], Gaël Chevallier[a], Charles Arnould[b], Eric Collard[b]

[a] *Univ. Bourgogne Franche-Comté - FEMTO-ST Institute*
Dpt of Applied Mechanics, 24, chemin de l'Epitaphe, 25000 Besancon, France
[b] *THALES LAS France, 2, avenue Gay Lussac, 78990, Elancourt, France*
[c] *ISAE-Supméca, Laboratoire QUARTZ EA 7393 - 3 rue Fernand HAINAUT - 93400 Saint-Ouen, France*

Abstract

Tuned Mass Dampers (TMD) are passive devices well-known to mitigate vibrations thanks to the principle of vibration absorption. They consist of a mass, a spring and a damper whose frequency is tuned to a critical frequency of a master structure in order to generate the expected energy transfer. As these devices require a very fine tuning to be efficient, Multi-frequency designs (Multiple Tuned Mass Dampers - MTMD) integrating several absorbers whose specific frequencies are distributed around the target resonance frequency have emerged to obtain good damping performances on a wide frequency band, even in the presence of uncertainties. The elastodynamic properties of these designs are classically estimated from lumped mass models that are a simplified representation of the 3D structures that will actually be used on a real application. In this context, the purpose of the paper is to design a metabsorber consisting in a set of 3D resonators, and to estimate numerically and experimentally the performance and the robustness in an uncertain context. The design approach relies on a dynamic analysis of the whole structure using the Finite Element Method that allows to considerate any topology for the absorbers. Epistemic uncertainties resulting from lack-of-knowledge on the target frequency are introduced, and the robustness of the metabsorber is estimated using the Info-Gap Theory that is a non-probabilistic approach for decision-making in such an uncertain context. Different frequency distributions in the metabsorber are compared to quantify the gain in performance and robustness that can be achieved changing the number of absorbers. The methodology is applied to the case of a simplified airplane model in order to control the third bending mode : numerical and experimental result show that even if the robustness

improves when the number of different absorbers increases, very good results can be obtained by using a reduced number of absorbing elements in the metabsorber.

Keywords: Multiple Tuned Mass Damper, Absorption, Lack-Of-Knowledge, Robustness, Passive Damping, Info-Gap Theory

2021 MSC: XX-XX, XX-XX

1. Introduction

Vibratory energy absorption is the working principle of Tuned Mass Dampers (TMD), also known as Dynamic Vibration Absorbers to passively mitigate vibrations. The use of TMD in order to control the vibrations of a structure around a given frequency consists in attaching a secondary device with a resonant frequency tuned to match that of the main structure. At the design frequency, an energy transfer operates from the structure to the TMD and allows to attenuate vibrations. The concept of Multiple Tuned Mass Dampers (MTMD) is to implement a set of TMD rather than a single one in order to, among other things, reduce the mass of each TMD and limit the space required. It may be noted that the same concept of absorption is exploited in the recent development of Resonant MetaMaterials (RMM) where local resonators are periodically attached to or integrated within the main structure to generate energy transfer or trapping between the structure and these secondary devices [1, 2, 3]. There is a vast literature on RMM, also referred to as Elastic MetaMaterials or metastructures for metamaterial-based finite structures, many different configurations have then been investigated such as discrete-like resonators consisting in spring-mass-dampers introduced on beams [4, 5, 6], plates [7, 8], cantilever-in-mass resonators [9], or tensioned-elastic membrane with mass blocks resonators [10]. The main interest in the case of metamaterials is that resonators generate local resonance bandgaps in a lower frequency range than the Bragg scattering phenomena which is linked to the spatial periodicity. TMD, MTMD as well as RMM are therefore based on the same principle of energy absorption, the main difference lies into the number and the size of absorbers. The advantage of using MTMD is that TMD are very sensitive to detuning, and perform poorly outside a narrow frequency band

*emeline.sadoulet-reboul@univ-fcomte.fr

around the frequency being monitored: this is known as the frequency detuning effect. The same effect occurs with MTMD when resonators are all tuned to the same frequency or in Resonant Metamaterial when perfectly periodic: the effective attenuation bandgap is deep but quite narrow and very sensitive to uncertainties. A strategy then consists in considering a frequency distribution in MTMD [11, 12, 13] in order to be more effective on a wider frequency band and more robust to detuning. By introducing multiresonators into metamaterials [14, 15, 16], or a hierarchical configuration [17], it is possible to generate multiple bandgaps and, with adequate design, to achieve broadband effectiveness by merging the separated bandgaps. By tuning the natural frequencies of the local resonators and structural parameters, Bragg and resonant bandgaps can be coupled for instance [18]. The design of functionally graded metamaterials, with spatially-varying properties in terms of material or geometry, allows to distribute the pass-bands and expand the attenuation bandwidth [19]. It is also interesting to note that a particular frequency distribution characterized by a high modal density around the natural frequency of the master structure allows to absorb near irreversibly the energy of the master structure [20, 21], and avoid the energy return generally observed with a finite number of oscillators [22]. Finally, all the studies done on energy absorption tend to show that multistructures, MTMD as resonant metamaterials, with distributed vibration absorbers are the best configuration to attenuate effectively on a frequency broadband.

The next question is thus to determine the optimal frequency distribution for a given problem. Many studies aim at finding the optimal frequency distribution to ensure performances in vibration control, but high performance is often obtained at the expense of robustness such that a trade-off between these two objectives has to be found. Robust optimization methods have been developed with uncertain parameters [23] or uncertain parameters and positions [24], modeled as stochastic variables, in order to minimize the mean or the stochastic vibratory response [25, 26]. Some strategies aim at considering both the control performance and the robustness by solving a two-objective optimization problem with a genetic algorithm [27] or by adding a frequency bandwidth ratio with a weighting factor into the performance index [28]. The question of robustness of multi-frequency metastructures has received less attention to the author's knowledge [29, 30]. In [31], the varia-

tion of mechanical parameters for the resonator modifies the limits of the band-gaps. The break of periodicity due to variability in additive manufacturing is investigated in [32, 33, 34]: detuned resonators can change the attenuation performance even for small levels of variability, and suppress as well as widen band-gaps.

Many of the studies done on MTMD or on RMM rely on lumped mass models that are easier to simulate, and that lead to reduced computational times [3, 35]. These models allow to identify the elastodynamic properties of the absorbers, but they need to be improved to take into account the real topology of the absorbers composing the metastructure, or their position that has an impact on the effectiveness. For instance, recent works on spatially distributed TMD show that it is necessary to introduce the effective mass of a structure to evaluate the efficiency of the absorbers [36], meaning that the absorber position is an influent parameter. The proposed paper details a methodology to design a metabsorber consisting in a set of 3D resonators, and the purpose is to investigate the performance and the robustness of the structure when changing the number of resonators and for the same added mass. The variability taken into account is a variation of the frequency to control that can be due to changes in the environmental conditions, ageing of materials, assembly conditions among others. No probabilistic description of the uncertain variables is available in this case, and stochastic approaches are inadequate. This is considered as lack-of-knowledge, an epistemic uncertainty for which a large amount of information is missing. The robustness is thus evaluated using the Info-Gap theory [37] that is a non-probabilistic approach adapted for cases where no probabilistic description of parameters is available. This approach is a decision-making tool in a context of epistemic uncertainty that has already been applied for identification of an appropriate model in presence of lack-of-knowledge [38], to study the collapse resistance of structures under uncertain loads [39], or to quantify the damping performances of viscoelastic materials in an uncertain temperature environment [40]. The methodology is here applied to study a metabsorber designed to control the third bending mode of a simplified airplane model. The paper is organized as follows: a deterministic optimization of the metabsorber is proposed in Section 2 using a Finite Element Model of the whole structure. Different configurations are tested

for which the number of resonators changes while keeping the same mass. Section 3 is dedicated to the robustness analysis of the deterministic optimal designs using the Info-Gap Theory, and the question is to compare the robustness efficiency obtained as a function of the number of resonators in the distribution. Finally, experimental validations are presented in Section 4, and conclusions are summarized in Section 5.

2. Optimal design of a metabsorber

Consider a main structure with a vibration mode to be controlled over a frequency band of interest. As an example, Fig.1 presents a CAD design of an airplane model presenting vibrations to control on the third bending mode. The airplane is composed of a main fuselage in aluminum, a through-wing and horizontal and vertical stabilizers in steel. The wing and the stabilizers are fixed on the fuselage thanks to angle bars in aluminum. All the geometrical and material parameters for the studies are recalled in Appendix A. This example will be used as an application case to illustrate the proposed methodology.

The control of the bending mode is done using a metabsorber composed of a set of N absorbers (Fig.2): each absorber consists in a beam as in [20], but to generalize the methodology to any kind of absorber, it will be modeled as a 3D component using the Finite Element Method. The device is attached at candidate position which is the most favorable one to attach the single TMD. It is made with PMMA whose properties are given in Appendix A. As a starting configuration all the elements are assumed to be identical, their varying properties will be determined thanks to optimization strategies in the next sections.

As the effectiveness of the absorbers depends on their number, their spatial distribution on the main structure, and is linked to the modal behaviors, the developed tools are based on a numerical dynamic analysis of the finite structure [41].

2.1. Finite Element Model of the master structure with the metabsorber

The FE method is used to study the dynamic behavior of the whole structure. The mesh is composed of quadratic tetrahedral elements and of quadratic brick elements on the metabsorber,

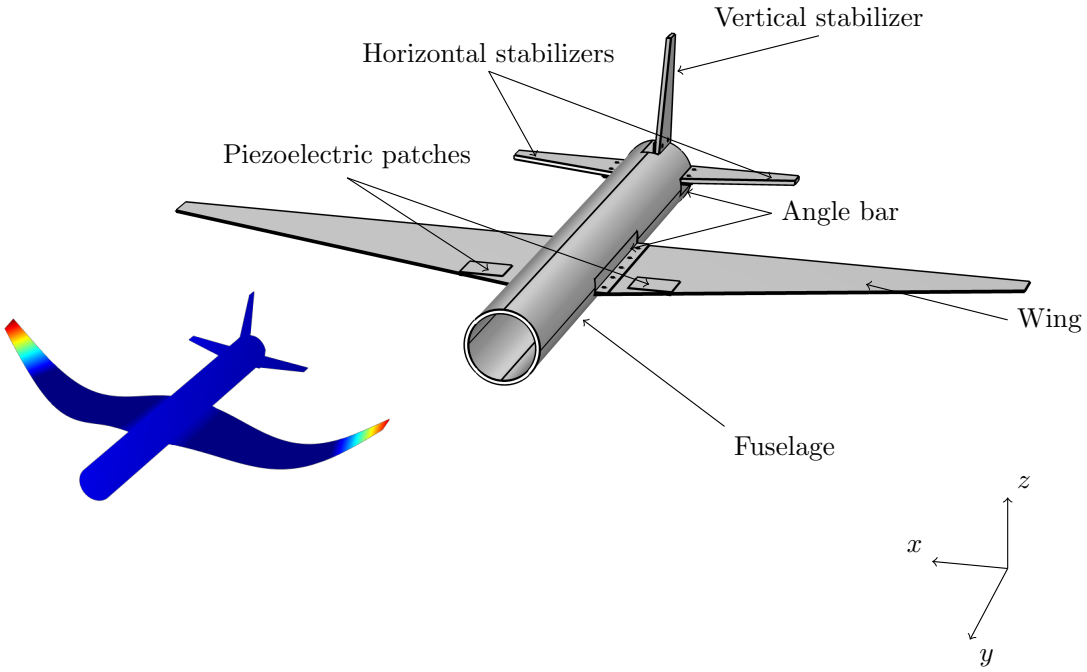

Fig. 1: The primary structure consists in an airplane model composed of a main fuselage, a through-wing and horizontal and vertical stabilizers. The wings and the stabilizers are fixed on the fuselage thanks to bar angles. Two couples of piezoelectric transducers are introduced in the model to match the experimental configuration presented in section 4. The study focuses on the control of the third bending vibration mode, illustrated by the figure on the left.

with a total of 164550 dofs. The equations governing the dynamic behavior of the whole structure including the airplane and the metabsorber in the frequency domain can be written as,

$$\left(\mathbf{K}^* - \omega^2 \mathbf{M}\right) \hat{\mathbf{U}} = \hat{\mathbf{F}}, \tag{1}$$

where $\mathbf{K}^*$ and $\mathbf{M}$ are respectively the complex stiffness and the real constant mass matrix of the structure, $\hat{\mathbf{U}}$ is the complex displacement vector and $\hat{\mathbf{F}}$ is the excitation vector. The complex stiffness can be written as,

$$\mathbf{K}^* = \mathbf{K}^*_{\mathbf{s}} + \mathbf{K}^*_{\mathbf{abs}}, \tag{2}$$

involving the complex stiffness $\mathbf{K}^*_{\mathbf{s}}$ of the main structure and the complex stiffness $\mathbf{K}^*_{\mathbf{abs}}$ of the absorbers. The complex nature of the matrices is linked to the consideration of loss factors in-

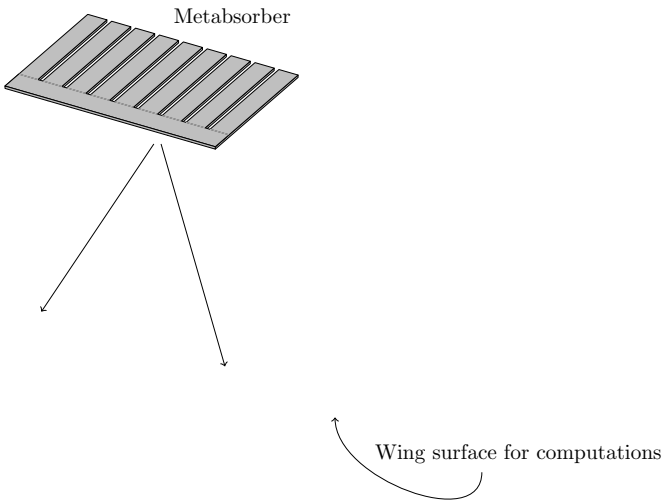

Fig. 2: Design of the metabsorber and integration on the airplane wing : The metabsorber consists in a set of beam-like absorbers attached on the wing of the airplane to control: the configuration is here presented for a uniform distribution such that all the beams have the same length. Computations are done on the wing surface opposite to the metabsorber.

troduced to model structural damping in the main structure η, and in the absorbers η_{abs}. In this configuration the size of the vector to compute is the number of degrees of freedom in the Finite Element Model. To reduce computational costs it is possible to use a reduction basis made of the eigenmodes. Loss factors are assumed to be small enough to consider that the normal modes of the linear conservative system are not changed much and can be used for the basis. Under this assumption the modal basis $\mathbf{\Phi} = [\phi_\mathbf{1}\, \phi_\mathbf{2}\, \cdots\, \phi_\mathbf{p}]$ composed of the p first eigenmodes is introduced and computed as,

$$\left(\mathbf{K} - \omega_\mathbf{p}^\mathbf{2}\mathbf{M}\right)\phi_\mathbf{p} = \mathbf{0}, \tag{3}$$

where $\mathbf{K}$ is the real part of $\mathbf{K}^*$. The dynamic equations for the reduced model are thus written as,

$$\left(\mathbf{k}^* - \omega^\mathbf{2}\mathbf{m}\right)\hat{\mathbf{q}} = \hat{\mathbf{f}}, \tag{4}$$

where $\mathbf{m} = \mathbf{\Phi^T M \Phi}$, $\mathbf{k}^* = \mathbf{\Phi^T K^* \Phi}$ and $\hat{\mathbf{f}} = \mathbf{\Phi^T}\hat{\mathbf{F}}$ are the projected operators. $\hat{\mathbf{q}} = \mathbf{\Phi^T}\hat{\mathbf{U}}$ are the generalized coordinates. $\mathbf{k}^*$ is the sum of $\mathbf{k}_\mathbf{s}^*$ that is the reduced matrix for the main structure, and of $\mathbf{k}_\mathbf{abs}^*$ that is the reduced matrix for the absorbers.

2.2. Optimization methodology

Firstly, a deterministic optimization is performed in order to find a reference distribution for the natural frequencies of the metabsorber. It is proposed to consider as design variables the stiffness properties for the N absorbers attached: indeed, the damping properties introduced on the absorbers are difficult parameters to modify in the design; thus the structural damping is fixed at the value of 6.6% which corresponds to what has been identified from an experimental test using an Oberst approach (ASTM E 756-98). The added mass is required to be small and will be fixed at about 18 g that corresponds to 4.5% of the wing mass (equal to 403 g). The strategy to control the absorbers' stiffness consists in introducing a coefficient α_i ($1 \leq i \leq N$), and the corresponding topology will be identified in a second step. By changing the number of different α_i, it is possible to study different metabsorber configurations, while working with the same mass assumption : for instance, the case where all the α_i are equals corresponds to a uniform distribution and can be assimilated to an equivalent single TMD (1-TMD), the case where all the α_i are different corresponds to a N-TMD metabsorber. The reduced matrix stiffness is thus modified as follows,

$$\mathbf{k_{abs}} = \sum_{\mathbf{i=1}}^{\mathbf{N}} \alpha_\mathbf{i} \mathbf{k^i_{abs}}, \tag{5}$$

where $\mathbf{k^i_{abs}}$ is the stiffness matrix of the ith absorber. The distribution of the α_i-parameters is representative of the squared natural frequencies of the MTMD absorbers. Different optimization objective functions can be defined, it is chosen here to focus on the minimization of the elastic strain energy of the airplane structure on a frequency band around the resonant frequency to control. This energy is a global quantity that ensures that the MTMD will be efficient on all the structure and will not only reduce locally the vibration amplitude. Moreover, the computational time required to estimate this quantity is low when working with projected operators. For an harmonic excitation, the average strain energy over the vibration period is defined using the reduced operators as,

$$E(\omega, \alpha_i) = \frac{1}{4} \hat{U}(\omega, \alpha_i)^H K_s \hat{U}(\omega, \alpha_i) = \frac{1}{4} \hat{q}(\omega, \alpha_i)^H k_s \hat{q}(\omega, \alpha_i) \tag{6}$$

where H denotes the hermitian or conjugate transpose. The optimization problem can thus be written as,

Given	ω_{min}, ω_{max}, $\alpha_{\min}$, $\alpha_{\max}$
Find	α_i, $1 \leq i \leq N$
Minimizing	$\int_{\omega_{min}}^{\omega_{max}} E(\omega, \alpha_i)\, d\omega$
Subject to	$\alpha_{\min} \leq \alpha_i \leq \alpha_{\max}$

where ω_{min} and ω_{max} are frequencies respectively below and above the frequency to be controlled. The lower and upper bounds for the parameters are arbitrary defined as $\alpha_{min} = 0.5$ and $\alpha_{max} = 1.5$, and the parameters are initially fixed to 1. The optimization problem is solved using the fmincon function available in mathematical software package MATLAB.

2.3. Application - Optimization results

The metabsorber considered in this work consists in two sets of 9 absorbers. The structure is almost symmetrical, but not exactly because of the angles used for the assembly, and it is chosen to consider each of the 18 absorbers independently. The frequency band of interest is between $\omega_{min} = 60\,\text{Hz}$ and $\omega_{max} = 90\,\text{Hz}$, around the frequency of the third bending mode for the plane. $p = 30$ modes are taken into account in the modal basis.

2.3.1. Optimization results for the 1-TMD case

The optimization is firstly done considering the uniform case for which all the beams in the metabsorber have the same length. This configuration gives rise to an equivalent single TMD. Starting from a unit initial value and an initial beam length $L = 8.5\,\text{cm}$, the coefficient obtained at the end of the optimization process is $\alpha = 1.01$. Fig. 3 presents the average of the receptance norms computed on the wing surface (Fig. 2). It can be observed a slight unbalance compared to the equal-peak method classically used for TMD-design. This is an influence of the structure which has several modes and non-uniform damping properties, such that an equal-peak design requires a specific optimization procedure as described in [42].

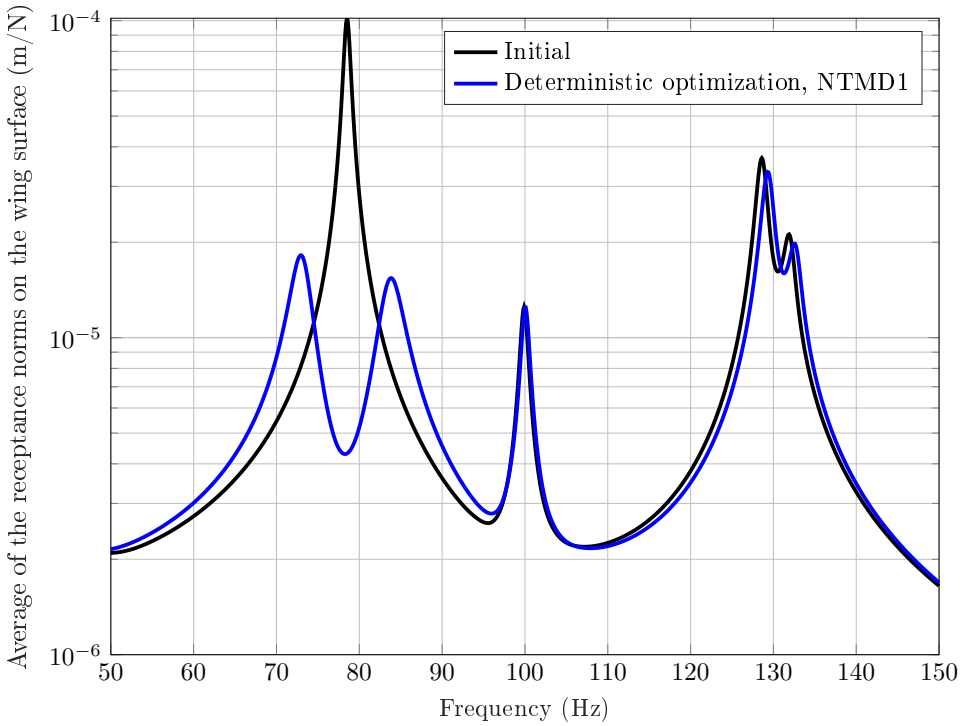

Fig. 3: Average of the receptance norms on the wing surface for the initial airplane and for the airplane with metabsorber NTMD1 that contains identical absorbers. (Legend color on the web version of the article)

2.3.2. Optimization results for the 1-TMD to the N-TMD case

The optimization study is then done changing the configuration of the metabsorber. Five cases are considered, by changing the number of different lengths, and thus the frequency distribution (Tab.1).

Case	Number of different lengths	Coefficients α
NTMD2	2	$\alpha_{1:2:17} \neq \alpha_{2:2:18}$
NTMD3	3	$(\alpha_{1:3:16} \neq \alpha_{2:3:17} \neq \alpha_{3:3:18})$
NTMD6	6	$(\alpha_{1:6:13} \neq \alpha_{2:6:14} \neq \alpha_{3:6:15} \neq \alpha_{4:6:16} \neq \alpha_{5:6:17} \neq \alpha_{6:6:18})$
NTMD9	9	$(\alpha_{1,10} \neq \alpha_{2,11} \neq \alpha_{3,12} \neq \alpha_{4,13} \neq \alpha_{5,14} \neq \alpha_{6,15} \neq \alpha_{7,16} \neq \alpha_{8,17} \neq \alpha_{9,18}$.
NTMD18	18	All the coefficients are different.

Table 1: Properties of the different metabsorbers studied by changing the number of beams with different lengths.

The distribution of the α_i parameters obtained at the end of the optimization process for each metabsorber configuration (NTMD1 to NTMD18) is presented on Fig.5b. The associated average of the receptance norms on the wing surface are given on Fig.4. It is also possible to represent the

variation of the stiffness properties of the absorbers in terms of frequency distribution considering a beam-model for the absorber, with clamped-free boundary conditions, and writing the natural frequency as $\omega^2 = \frac{\beta^2}{L^2}\sqrt{\frac{\alpha_i B}{m}}$ where B and m are the bending stiffness and the mass per unit length, and $\beta = 1.875$ for the first mode.

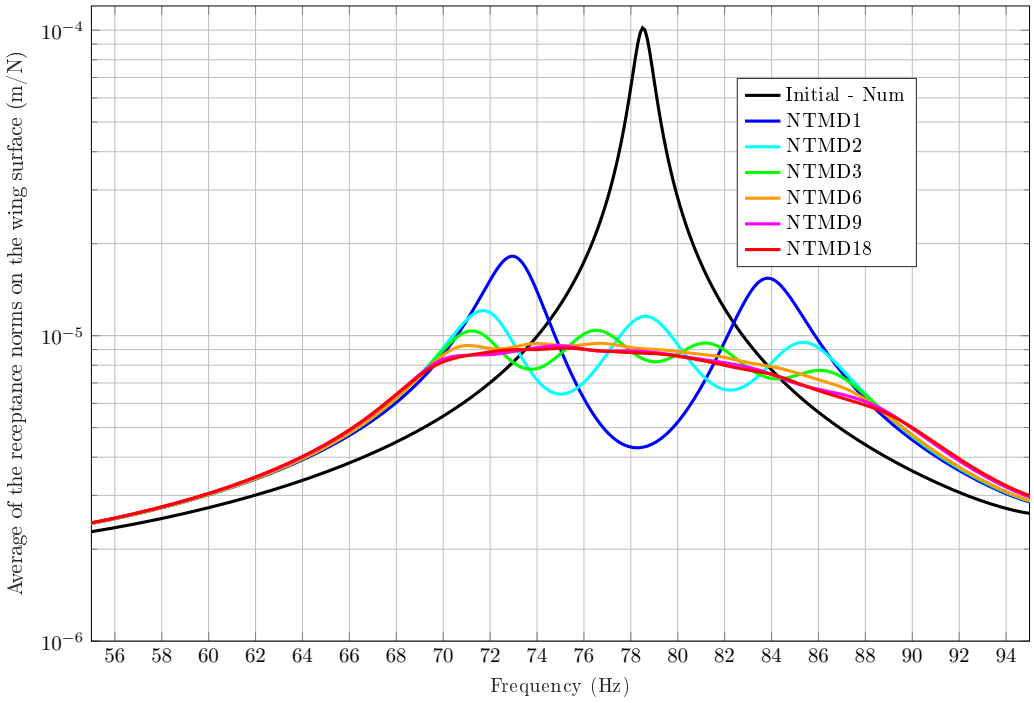

Fig. 4: Average of the receptance norms on the wing surface for the initial airplane and for the airplane with metabsorber NTMD1/2/3/6/9/18 (Legend color on the web version of the article)

It can be observed that the metabsorber significantly reduces the amplitude of the response on a wide range of frequencies around the frequency to control, and that the attenuation increases with the number of different absorbers in the device. The frequency distribution in the metabsorber tends to be almost linear around the tuned frequency and it is noticeable that there is no great gain in attenuation between the NTMD9 and NTMD18 configurations with the largest number of absorbers. The methodology proposed to design a metabsorber consisting in a set of 3D resonators is thus based on a modal basis reduction reduction approach, on a design by modifying the stiffnesses of the absorbers, and on the computation of energy quantities. Computational costs are

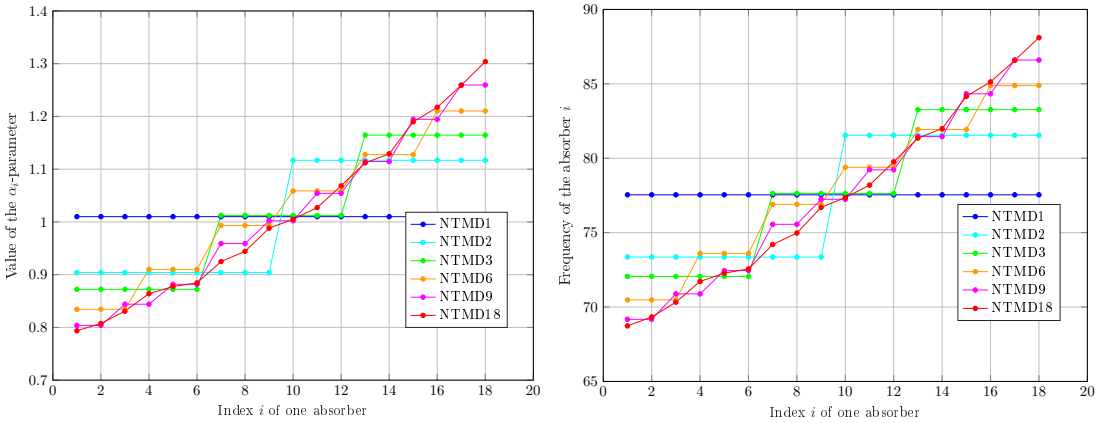

(a) Distribution of the α_i-parameters ($1 \leq i \leq 18$)

(b) Frequency distribution

Fig. 5: Structure of the metabsorbers (NTMD1/2/3/6/9/18) after the optimization process (Legend color on the web version of the article)

reduced as the optimization process takes only a few seconds. By this way, it has been possible to define networks adapted to a complex 3D structure. The purpose is now to compare the robustness of the devices under lack-of-knowledge.

3. Robustness analysis of the optimal metabsorber design

The optimal design parameters have been determined in section 2 without uncertainties, the purpose of this section is to evaluate the robustness of the designs when the frequency to control for the master structure is poorly known or varies. Indeed, during the structure life, the distribution of the embedded masses may vary, the environmental conditions may be modified leading to changes in the structure or material behaviors that may affect the frequency to be controlled. It is thus necessary to evaluate the robustness of the metabsorber to such variations, that is evaluate its ability to still mitigate vibrations in case of unknown uncertainties. The methodology here proposed is based on the Info-Gap decision theory that is a non-probabilistic decision theory under severe uncertainty [37]. It is particularly well suited when no probabilistic information is available, as in the case of frequency detuning considered in this paper. The theory relies on the introduction of three data: a model, a performance criterion, and an info-gap uncertainty model. Such a model consists in a family of nested sets, where each set corresponds to a level of uncertainty. The robustness analysis using this approach aims to determine from which level of lack-of-knowledge

the performance criterion is not verified anymore. In the present study, the model consists in a 3D numerical Finite-Element model used to estimate the performance of a metabsorber quantified from the reduction of vibratory energy that it allows. Lack-of-knowledge is introduced through perturbations of the mass matrix that result in a lack of knowledge about the frequency of the main structure to control. The following sections detail these concepts.

3.1. Estimation of the robustness using the Info-gap approach

Lack-of-knowledge on the master frequency to control is introduced on the reduced mass matrix $\mathbf{m}$ of the master structure through the matrix $\mathbf{dm}$ that represents the perturbation of the modal mass matrix due to the added lumped mass in the experiments. $\mathbf{m_{2\times 2}}$ is the full mass matrix that takes the lumped mass into account while $\mathbf{m}$ is the nominal full mass matrix:

$$\mathbf{dm} = \mathbf{\Phi}^T \left[\mathbf{m_{2\times 2}} - \mathbf{m}\right] \mathbf{\Phi} \tag{7}$$

In the simulations, the perturbation is also defined by the parameter γ_0 that allows to drive continuously the mass, and consequently the frequency uncertainties. Hence, the dynamic equation Eq. (4) is written as,

$$\left(\mathbf{k}^* - \omega^2 \left(\mathbf{m} + \gamma_0 \mathbf{dm}\right)\right) \hat{\mathbf{q}} = \hat{\mathbf{f}} \tag{8}$$

such that for the nominal value $\gamma_0 = 0$ the dynamic equation corresponds to the initial problem. The Info-Gap uncertainty model, in this case the envelope model, is given in Eq. (9),

$$U\left(h, \tilde{\gamma}_0\right) = \left\{\gamma_0 : \left|\gamma_0 - \tilde{\gamma}_0\right| \leq h\right\}, h \geq 0 \tag{9}$$

h is the horizon of uncertainty on the nominal value $\tilde{\gamma}_0$ of the matrix coefficient γ_0. At any level of uncertainty h, U contains all coefficients γ_0 whose distance from $\tilde{\gamma}_0$ is not greater than h. The performance of the metabsorber is estimated from the calculation of the ratio R_0^{MTMD} between

the elastic strain energy on the frequency band of interest with and without the metabsorber,

$$R_0^{MTMD} = \frac{E^{MTMD}}{E^0}, \tag{10}$$

where E^{MTMD} is the strain energy of the master structure estimated when the metabsorber is attached to the master structure and E^0 is the energy without metabsorber. When the efficiency of the metabsorber decreases, the ratio R_0^{MTMD} increases and tends to 1. The robustness function $\hat{h}$ is thus defined as the greatest horizon of uncertainty h, that is to say the greatest variation in the frequency to control, such that the worst case ratio (max) remains inferior to the critical value R_0^c,

$$\widehat{h}(R_0^c) = max \left\{ h : \left(\max_{\gamma_0 \in \mathcal{U}(h,\tilde{\gamma}_0)} R_0^{MTMD} \right) \leq R_0^c \right\} \tag{11}$$

As $\hat{h}$ gets larger, the sensitivity of the MTMD device to lack of knowledge gets smaller. In practice, the estimation of the robustness is done increasing the horizon of uncertainty ($\{h_1, h_2, \ldots, h_{n_h}\}$) and looking for the worst case design calculated as,

$$\hat{R}_{h_i}(h) = \max_{\gamma_0 \in U(h_i,\tilde{\gamma}_0)} R_0^{MTMD} \tag{12}$$

It is possible to estimate uncertainty values for which the performance criteria $R_0^{MTMD} \leq R_0^c$ is respected.

3.2. Numerical application

Fig.6 presents the robustness of the different metabsorbers NTMD1/2/3/6/9/18 as defined in Eq.(11). The uncertainty introduced on the mass of the master structure is translated in terms of an uncertainty on the natural frequency of the structure, the relationship is determined from a modal analysis. The maximum frequency variation is 18% here. The value obtained when the maximum horizon on uncertainty h is equal to 0 corresponds to the determinist optimal performance that is the best that can be achieved. It can be observed that the metabsorber NTMD1 is less efficient than the other ones, as observed on Fig.4. Then, as the uncertainty increases, the master frequency deviates more and more from the nominal value for which the metabsorbers have been tuned, and

the energy ratio increases. This means that the metabsorbers are less and less efficient. Let consider the case of a critical R_0^c equal to 20% as represented by the vertical line on Fig.6. Whatever the NTMD configuration, it is possible to ensure this performance if the uncertainty on the main frequency is less than 8% (horizontal line). Nevertheless, the robustness is improved for more complex configurations with more absorbers.

Considering the zeroing property defined as the case without allowed uncertainty, it is clear that NTMD18 outperforms other configurations with respect to the performance metric. Moreover, it is also the most robust configuration as the curve is above the others for any given level of uncertainty. This case can be considered as the dominant robust one among all configurations. Finally, it can be observed that it also corresponds to the best performing configuration for all levels of uncertainty.

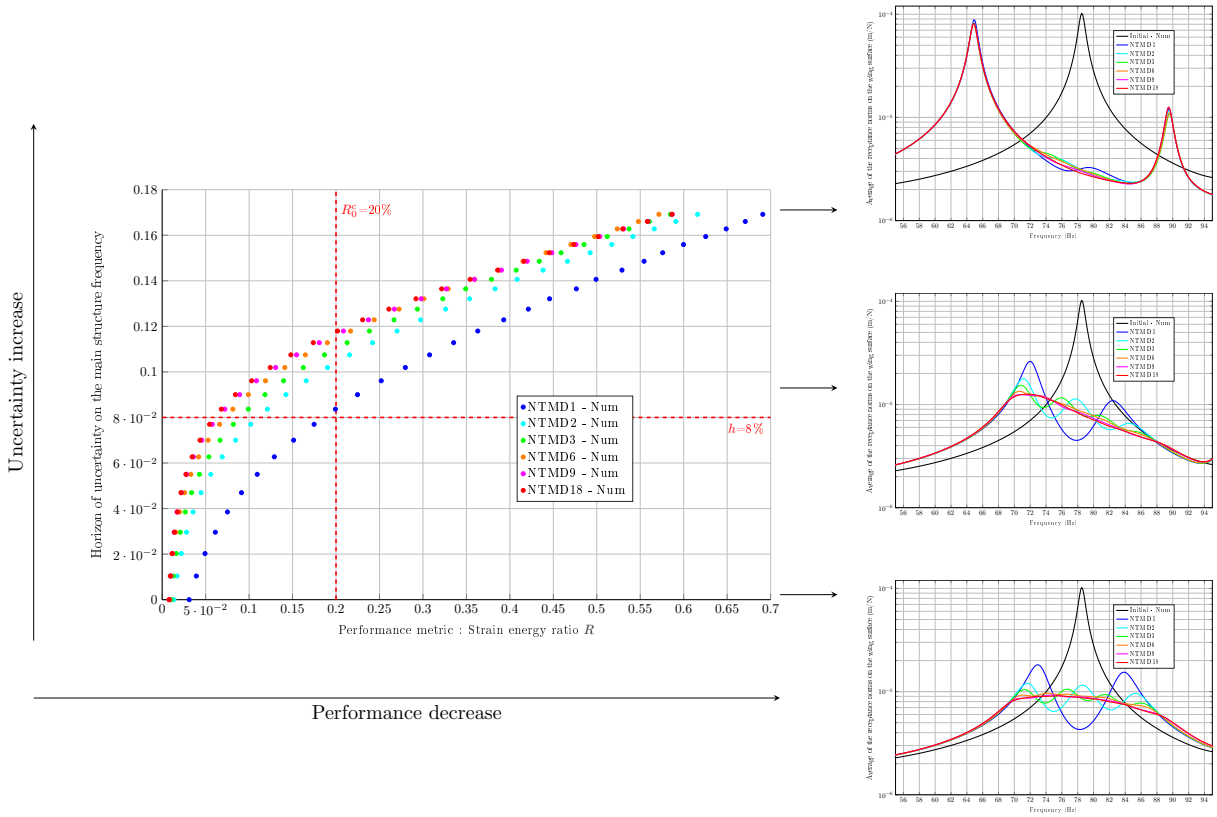

Fig. 6: Distribution of the robustness for metabsorber NTMD1/2/3/6/9/18 (Legend color on the web version of the article), the curves on the right represent the FRFs for three levels of uncertainty on the main frequency (horizon=0, 0.09 and 0.17).

4. Experimental analysis of the performance and of the robustness of the metabsorber

The purpose of this section is now to investigate experimentally the performances and robustness of the different metabsorbers, to validate the numerical design methodology, and to study the credibility of the robustness results obtained by numerical simulation in Section 3. The airplane as well as the metabsorber have been manufactured for an experimental validation of the methodology. The metabsorber is manufactured using a laser cutting machine from a 1.42 mm thick PMMA sheet. Fig.7a presents the airplane with one of the metabsorber prototypes glued on its wing. The different configurations studied for the metabsorbers (NTMD1/2/3/6/9/18) are presented on the same figure.

The airplane is free-free, suspended to a test frame thanks to flexible cables. It is excited by a sweep sine signal with two sets of piezoelectric patches (PIC 151, $3\,\text{cm} \times 3\,\text{cm} \times 0.5\,\text{mm}$) bonded on the wing (Fig.7b). The transverse velocity is measured on the wing surface using a Polytec Laser Doppler vibrometer: the experimental mesh contains $N_{exp} = 90$ test nodes.

4.1. Vibration measurements on the wing surface - Analysis in case of frequency shift on the main structure

Fig.8 presents the average of the receptance norms obtained experimentally on the wing surface without and with the 6 different metabsorbers (NTMD1/2/3/6/9/18). These results can be compared to the numerical ones presented in Fig.4 and quite a good agreement is observed with the emergence of a flat curve more regular as the frequency distribution in the metabsorber becomes more complex. In order to experimentally evaluate the impact of the metabsorbers when the frequency of the main structure changes, an addition of mass was realized by introducing magnets at the end of the wings. Two configurations are tested, in the first one a set of 2 magnets placed on both sides of the wing is introduced at each end (configuration called 2x2), in the second one a batch of 4 magnets is introduced (configuration called 4x4). Numerically, these added masses lead to modifications of the mass matrix which becomes respectively $\mathbf{m_{2x2}}$ and $\mathbf{m_{4x4}}$ for each configuration: these modified matrices are used to numerically evaluate the dynamic response of the

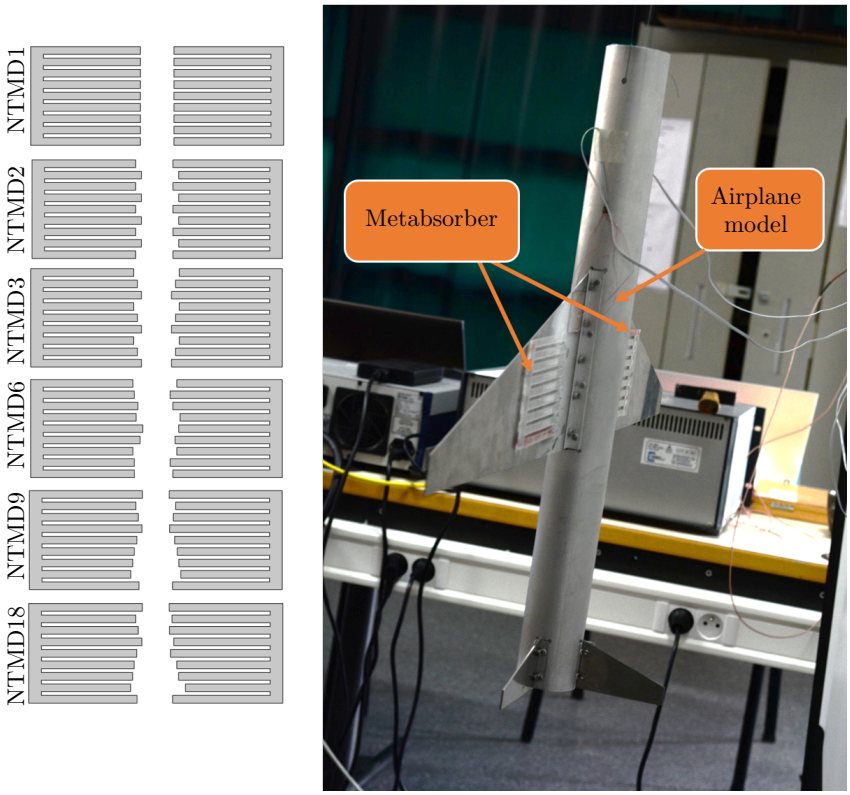

(a) Airplane model equipped with a metabsorber - Structure of the different metabsorber configurations NTMD1/2/3/6/9/18

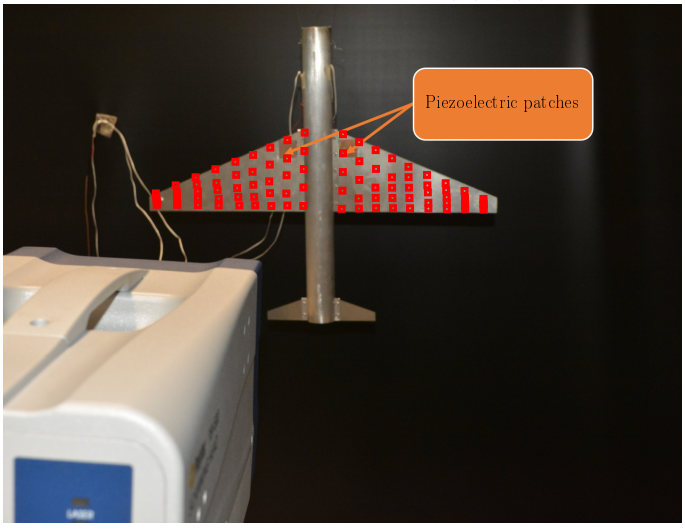

(b) The airplane is free-free, it is excited with two sets of piezoelectric patches. The transverse velocity is measured at 90 test nodes on the airplane wing using a Polytec Laser Doppler vibrometer.

Figure 7: Experimental set-up with the airplane model and the metabsorbers.

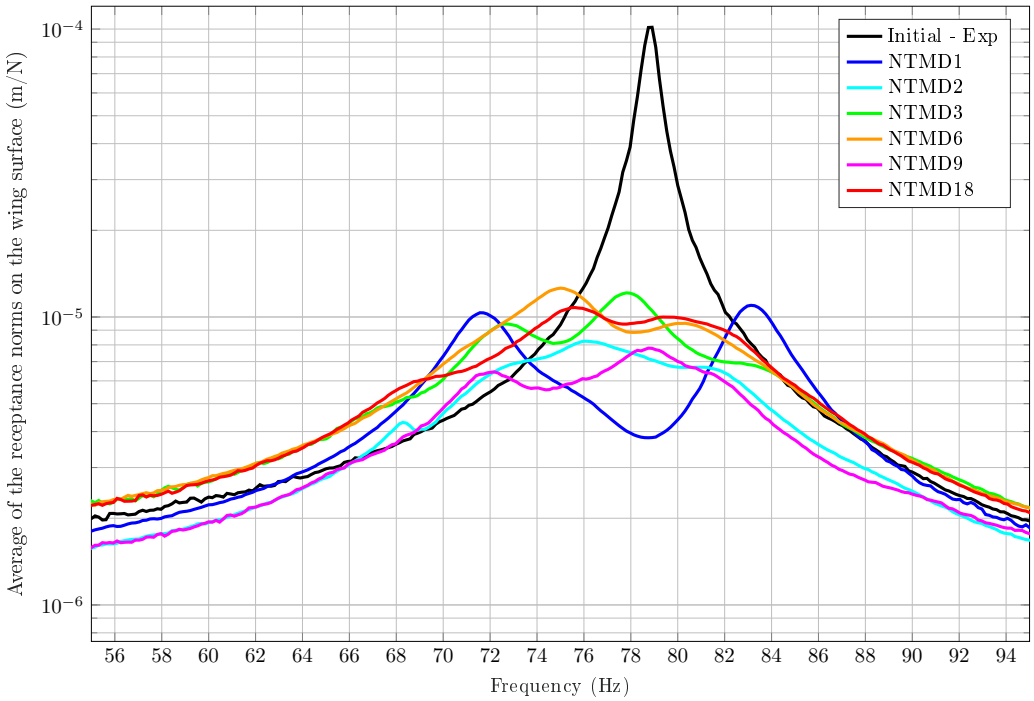

Fig. 8: Average of the experimental receptance norms on the wing surface for the initial airplane with metabsorber NTMD1/2/3/6/9/18 (Legend color on the web version of the article)

structure. The frequency shift induced on the studied mode is about 5.5% for case (2x2) and 9.6% for case (4x4). Experimentally, as before, the vibratory response of the wings was measured by laser vibrometry. Fig.9 presents the average of the receptances on the wings obtained numerically and experimentally in the case of the initial structure (called Initial - Num and Initial -Exp), and for the various metabsorbers without frequency shift (Ntmd - Num, Ntmd -Exp) and with the two configurations of frequency shift by added mass (Ntmd - 2x2, Ntmd - 4x4).

A first observation of the results shows that the experimental results are in good agreement with the numerical results for all configurations, which allows to validate the model used. For each case, the attenuation performance obtained with the metabsorbers decreases when a frequency shift is introduced on the main structure. A more accurate analysis shows that the loss of performance is greater for metabsorbers composed of similar absorbers. Thus the loss of efficiency for NTMD1 is greater than for NTMD18 since the maximum amplitude reached is higher. These results demon-

(a) NTMD1

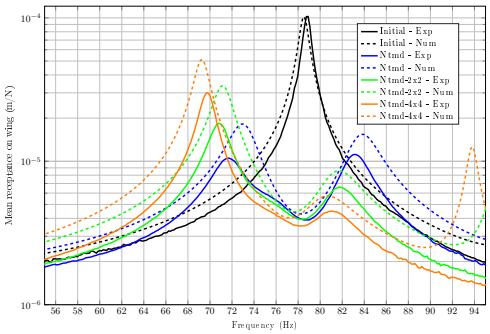

(b) NTMD2

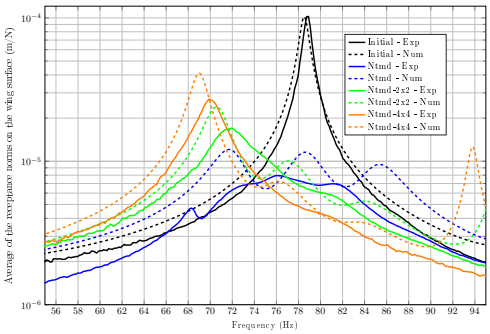

(c) NTMD3

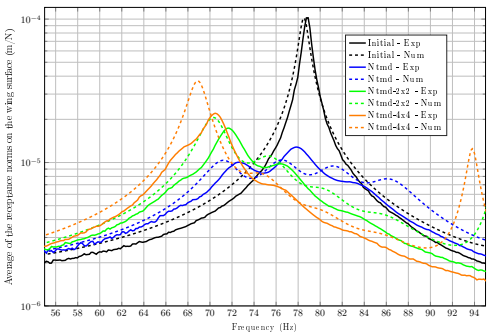

(d) NTMD6

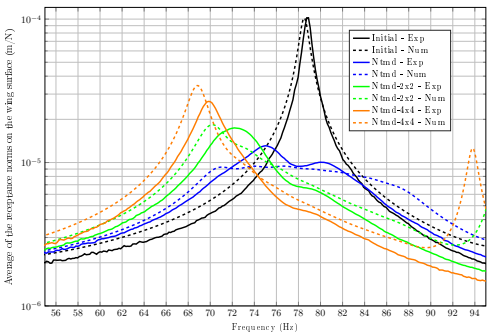

(e) NTMD9

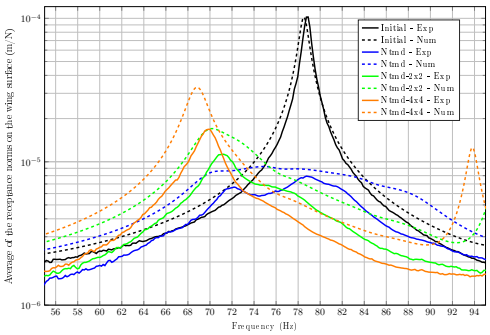

(f) NTMD18

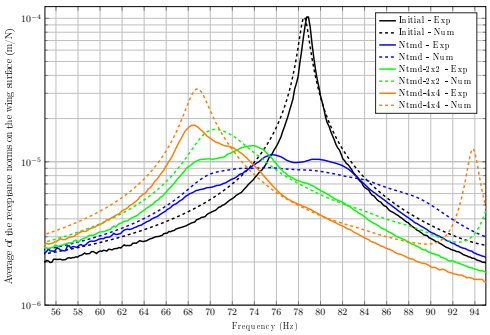

Figure 9: Average of the receptance norms on the wing obtained numerically and experimentally in the case of the initial structure (called Initial - Num and Initial -Exp), and for the various metabsorbers without frequency shift (Ntmd - Num, Ntmd -Exp) and with the two configurations of frequency shift by added mass (Ntmd - 2x2, Ntmd - 4x4) : (a) NTMD1, (b) NTMD2, (c) NTMD3, (d) NTMD6, (e) NTMD9, (f) NTMD18 (Legend color on the web version of the article).

strate a fact often cited in the literature that a multiple absorber is more robust than a single absorber. Besides, the NTMD2 metabsorber gives better results than probably expected: this is due to variabilities on manufacturing and properties that benefit in this case to performance. In order to deepen this conclusions, the objective now is to estimate this robustness in particular experimentally, and to position it with respect to the numerical estimates made with the info-gap method in section 3.

4.2. Performance estimation based on the experimental energy - Application of a modeshape experimental technique

The methodology proposed in section 3 to evaluate the robustness is based on the computation of the elastic strain energy on a frequency band of interest. In order to calculate the experimental energy following a method similar to that implemented numerically and thus using Eq. (6), it is necessary to determine the experimental generalized coordinates which are quantities that cannot be measured directly. The strategy proposed in this paper relies on a modeshape expansion technique [43] to estimate experimental coordinates from the measurements of receptances. The wing numerical modal basis $\mathbf{\Phi_{num}}$ is assumed to be known and is used to build an experimental modal basis $\mathbf{\Phi_{exp}}$ by interpolation of the N_{num} Finite Element Results on the N_{exp} test nodes. The size of the interpolated matrix is N_{exp} by N_{modes} where N_{modes} denotes the number of eigenmodes selected. In practice, measured quantities in this work are receptances, and the expansion method is such applied on these data. Experimental modal coordinates are estimated by transforming the measured receptances using the modal decorrelation,

$$\mathbf{\hat{q}_{exp}} = \mathbf{\Phi_{exp}}^{\mathbf{T}} \mathbf{\hat{H}_{exp}} \tag{13}$$

where $\mathbf{\hat{H}_{exp}}$ corresponds to the measured receptance. Assuming an harmonic excitation, a strain energy linked to the receptance is then computed as,

$$E_{FRF,exp} = \frac{1}{4} \mathbf{\hat{q}_{exp}^{H}} \mathbf{k_s} \mathbf{\hat{q}_{exp}}. \tag{14}$$

This energy can be related to the strain energy,

$$E_{\text{exp}} = E_{FRF,\text{exp}} \times \left\|\hat{\mathbf{f}}\right\|^2 \tag{15}$$

where $\left\|\hat{\mathbf{f}}\right\|^2$ is the square norm of the excitation force. As this norm is constant, and that the quantity of interest for the robustness study is an energy ratio as defined in Eq.(10), it is possible to work with this derivate energy. The residue of the modal expansion is defined as,

$$\mathbf{R} = \mathbf{\Phi_{exp}}\hat{\mathbf{q}}_{\mathbf{exp}} - \hat{\mathbf{H}}_{\mathbf{exp}}. \tag{16}$$

In order to illustrate the methodology, only the case of NTMD1 without frequency shift is presented in the paper. Fig.10a presents the average of the receptance norms measured on the wing, and obtained after expansion, and Fig.10b presents the absolute linear average residue error. The expansion is done here with 20 modes in the modal decomposition. It can be seen that the expanded results are overlaid with the measured results, at least on the first modes and on the frequency band of interest for the study. The error is very small, less than 10^-6, meaning that the proposed approximation is valid. Fig.11 depicts the strain FRF energy estimated using experimental modal

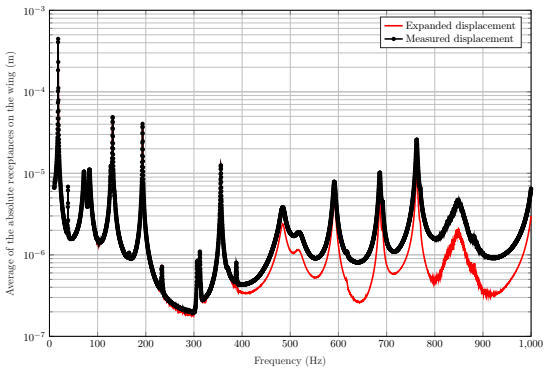

(a) Average of the receptance norms on the wing obtained with Measurements (black markers), Modal expansion (red line).

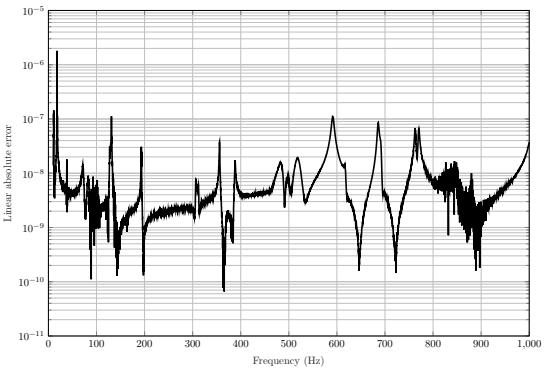

(b) Linear average error between the measured and the expanded displacements.

Figure 10: Approximation of the experimental results using a modal expansion method for the case of the airplane with metabsorber NTMD1

expansion on the frequency band between 60 Hz and 90 Hz for the initial airplane structure, and for the structure with metabsorber NTMD1 without frequency shift and with the two configurations of

frequency shift by added mass (Ntmd - 2x2, Ntmd - 4x4). The maximum energy over the frequency band can thus be estimated and the energy ratio used as a performance criterion can be deduced. Tab. 2 summarizes the results obtained for all the configurations tested.

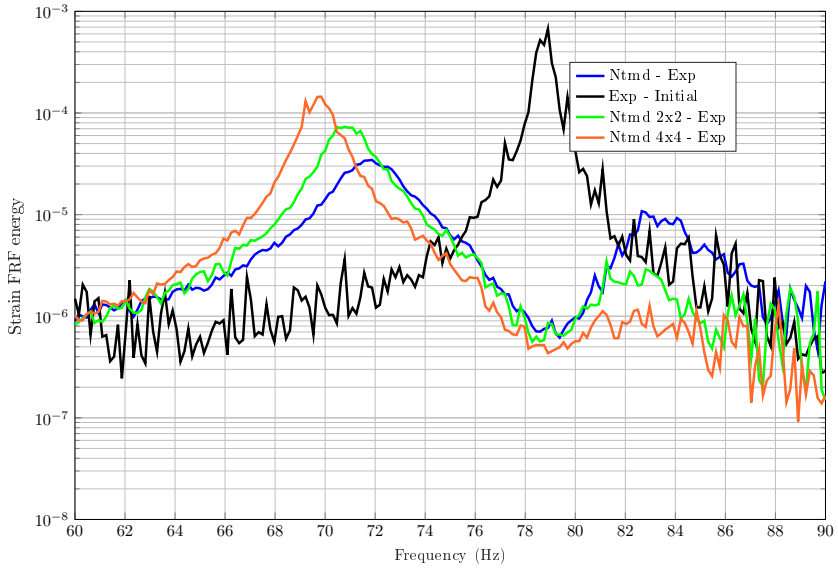

Fig. 11: Strain FRF energy estimated using experimental modal for the case of the airplane with metabsorber NTMD1 on the frequency band between 60 Hz and 90 Hz for the initial airplane structure (Exp - Initial), and for the structure with metabsorber NTMD1 without frequency shift (Ntmd - Exp) and with the two configurations of frequency shift by added mass (Ntmd - 2x2, 4x4) (Legend color on the web version of the article).

4.3. Analysis of the experimental robustness

Fig.12 and 13 present a comparison between the robustness of the metabsorbers estimated numerically using the Info-Gap approach, and the experimental robustness estimated using the expansion method for the initial design and for the two configurations of frequency shift. For the majority of cases the experimental robustness is as expected better than the numerical one as the Info-Gap approach predicts the worst case at any given level of performance.. Some isolated points are identified for NTMD1 and NTMD 6 where this conclusion is wrong: the proposed explanation for this is that the numerical method only considers uncertainties on the main structure, while in practice they exist everywhere, and in particular on the metabsorber due to manufacturing errors, material inhomogeneities, ... When these cannot be neglected as probably for the specific points in

Configuration	Without shift	With shift 2x2	With shift 4x4
NTMD1	0.0501	0.1079	0.2142
NTMD2	0.0069	0.0331	0.0431
NTMD3	0.0128	0.0301	0.0322
NTMD6	0.0283	0.0466	0.1180
NTMD9	0.0044	0.0050	0.0122
NTMD18	0.0073	0.0125	0.0213

Table 2: Ratio between the maximum energy with each metabsorber on the frequency band [60 Hz 90 Hz] and the maximum energy on the initial structure - without frequency shift and with the two configurations of frequency shift by added mass (Ntmd - 2x2, Ntmd - 4x4). The FRF strain energy for the initial structure used as a reference is $E^0 = 6.6972 \times 10^{-4}\,\mathrm{J\,N^{-2}}$.

Fig.12a and Fig.13a, it would require to complexify the approach taking two sources of uncertainties all together. Finally, the results demonstrate globally that a multiple configuration increases the level of robustness as the uncertainty increases, and a stabilization effect can be observed.

5. Conclusions

This paper proposes an approach to design a metabsorber consisting in a set of 3D resonators tuned to control a vibrating structure, and to study both numerically and experimentally its robustness in case of lack-of-knowledge on the frequency to control. The 3D configuration allows to consider complex topologies modeled using the Finite Element Method, adapted to real structures. The design methodology is applied to control a bending mode for an airplane model. Different frequency distributions are investigated to compare the performance and the robustness of the metabsorbers. An Info-Gap analysis is performed to quantify robustness by introducing lack-of-knowledge on the frequency to be controlled, without knowledge of probability distribution for this parameter. The investigated performance metric or this study is the strain energy on a frequency band around the frequency to control, which is a computationally inexpensive global quantity using reduced modal operators. The studied metabsorbers are realized and measurements by laser velocimetry allow to evaluate the performances of the different configurations. A modal expansion method is implemented to estimate the strain energy from the vibration measurements, and evaluate the robustness of each metabsorber. Finally, a frequency detuning of the main structure is introduced by adding weights on the wing tips. It is observed that the energy obtained experimentally without uncertainties corresponds to the numerically predicted energy. Moreover, the experimentally evaluated robustness is found for some lucky configurations to be better than the worst case estimated by the info-Gap approach, and follows the worst case trend for less robust configurations. Overall the robustness of the metabsorbers is better for more complex distributions for which the resonators vibrate at different frequencies, but it is notable that a saturation effect emerges so that very good behaviors are obtained experimentally and numerically without detuning all the resonators of the secondary structure. This phenomenon is observed in a context where the damping on the absorbers is high, the benefit of detuning the absorbers would certainly be more important for a lower damping.

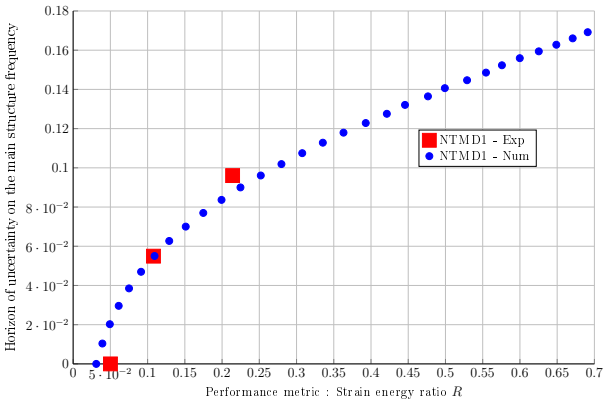

(a) NTMD1

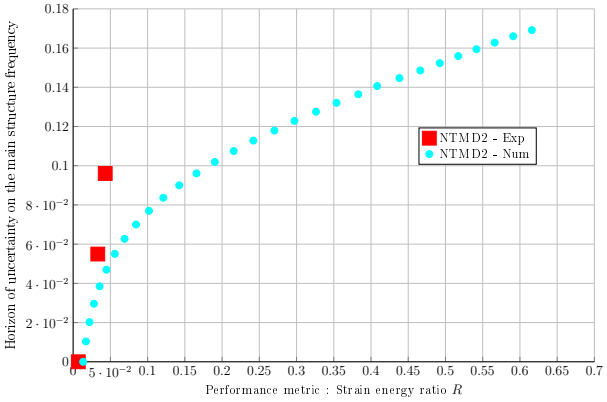

(b) NTMD2

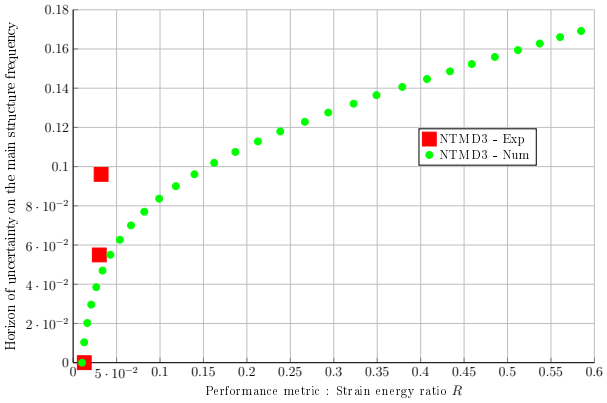

(c) NTMD3

Figure 12: Distribution of the numerical and experimental robustness for metabsorber NTMD1/2/3 (Legend color on the web version of the article)

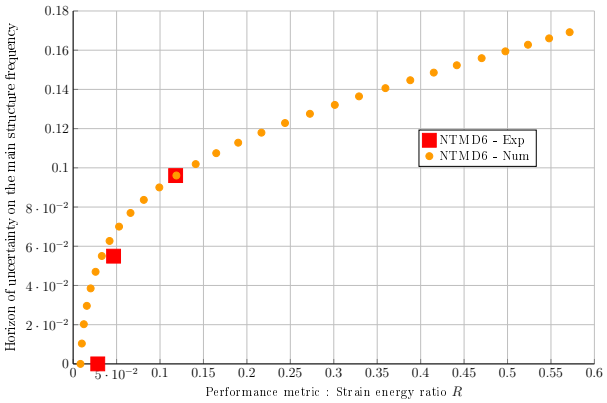

(a) NTMD6

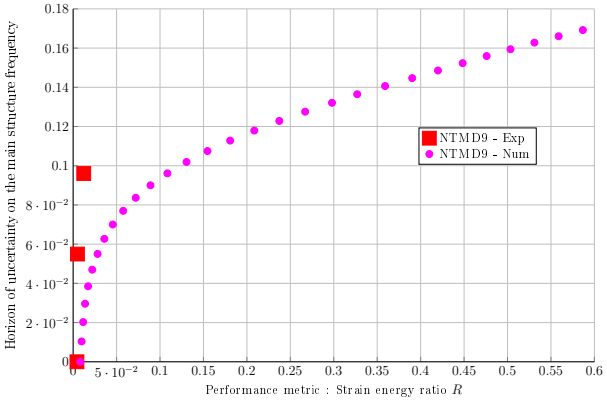

(b) NTMD9

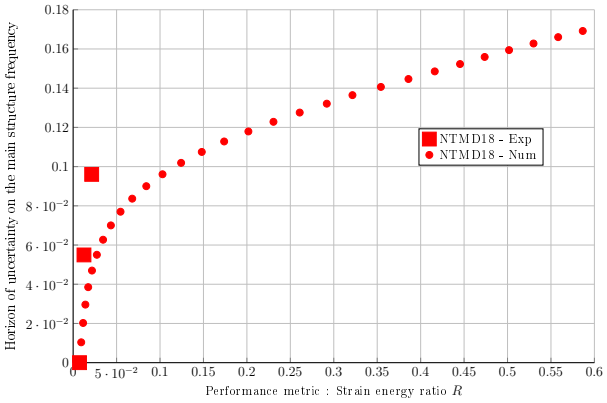

(c) NTMD18

Figure 13: Distribution of the numerical and experimental robustness for metabsorber NTMD6/9/18 (Legend color on the web version of the article)

Acknowledgements

This work has been supported by the EUR EIPHI Project (contract ANR-17-EURE-0002), Bourgogne Franche-Comté Region and the ANRT (CIFRE). Authors are grateful to the french company THALES LAS France for their financial support.

References

[1] Z. Liu, X. Zhang, Y. Mao, Y. Zhu, Z. Yang, C. T. Chan, P. Sheng, Locally resonant sonic materials, science 289 (5485) (2000) 1734–1736. doi:https://doi.org/10.1126/science.289.5485.1734.

[2] P. F. Pai, Metamaterial-based broadband elastic wave absorber, Journal of Intelligent Material Systems and Structures 21 (5) (2010) 517–528. doi:https://doi.org/10.1177/1045389X09359436.

[3] K. K. Reichl, D. J. Inman, Lumped mass model of a 1d metastructure for vibration suppression with no additional mass, Journal of Sound and Vibration 403 (2017) 75–89. doi:https://doi.org/10.1016/j.jsv.2017.05.026.

[4] D. Yu, Y. Liu, G. Wang, H. Zhao, J. Qiu, Flexural vibration band gaps in timoshenko beams with locally resonant structures, Journal of applied physics 100 (12) (2006) 124901. doi:https://doi.org/10.1063/1.2400803.

[5] H. Sun, X. Du, P. F. Pai, Theory of metamaterial beams for broadband vibration absorption, Journal of Intelligent Material Systems and Structures 21 (11) (2010) 1085–1101. doi:https://doi.org/10.1177/1045389X10375637.

[6] T. Wang, M.-P. Sheng, Q.-H. Qin, Multi-flexural band gaps in an euler–bernoulli beam with lateral local resonators, Physics Letters A 380 (4) (2016) 525–529. doi:https://doi.org/10.1016/j.physleta.2015.12.010.

[7] Y. Xiao, J. Wen, X. Wen, Flexural wave band gaps in locally resonant thin plates with periodically attached spring–mass resonators, Journal of Physics D: Applied Physics 45 (19) (2012) 195401. doi:https://doi.org/10.1088/0022-3727/45/19/195401.

[8] C. C. Claeys, K. Vergote, P. Sas, W. Desmet, On the potential of tuned resonators to obtain low-frequency vibrational stop bands in periodic panels, Journal of Sound and Vibration 332 (6) (2013) 1418–1436. doi:https://doi.org/10.1016/j.jsv.2012.09.047.

[9] A. Qureshi, B. Li, K. Tan, Numerical investigation of band gaps in 3d printed cantilever-in-mass metamaterials, Scientific reports 6 (2016) 28314. doi:https://doi.org/10.1038/srep28314.

[10] H. Zhang, Y. Xiao, J. Wen, D. Yu, X. Wen, Flexural wave band gaps in metamaterial beams with membrane-type resonators: theory and experiment, Journal of Physics D: Applied Physics 48 (43) (2015) 435305. doi:https://doi.org/10.1088/0022-3727/48/43/435305.

[11] K. Xu, T. Igusa, Dynamic characteristics of multiple substructures with closely spaced frequencies, Earthquake Engineering & Structural Dynamics 21 (12) (1992) 1059–1070. doi:https://doi.org/10.1002/eqe.4290211203.

[12] A. Kareem, S. Kline, Performance of multiple mass dampers under random loading, Journal of structural engineering 121 (2) (1995) 348–361. doi:https://doi.org/10.1061/(ASCE)0733-9445(1995)121:2(348).

[13] J. Park, D. Reed, Analysis of uniformly and linearly distributed mass dampers under harmonic and earthquake excitation, Engineering Structures 23 (7) (2001) 802–814. doi:https://doi.org/10.1016/S0141-0296(00)00095-X.

[14] G. Huang, C. Sun, Band gaps in a multiresonator acoustic metamaterial, Journal of Vibration and Acoustics 132 (3) (2010). doi:https://doi.org/10.1115/1.4000784.

[15] P. F. Pai, H. Peng, S. Jiang, Acoustic metamaterial beams based on multi-frequency vibration absorbers, International Journal of Mechanical Sciences 79 (2014) 195–205. doi:https://doi.org/10.1117/12.2045061.

[16] H. Chen, X. Li, Y. Chen, G. Huang, Wave propagation and absorption of sandwich beams containing interior dissipative multi-resonators, Ultrasonics 76 (2017) 99–108. doi:https://doi.org/10.1016/j.ultras.2016.12.014.

[17] K. Billon, I. Zampetakis, F. Scarpa, M. Ouisse, E. Sadoulet-Reboul, M. Collet, A. Perriman, A. Hetherington, Mechanics and band gaps in hierarchical auxetic rectangular perforated composite metamaterials, Composite Structures 160 (2017) 1042–1050.

[18] S. Hao, Z. Wu, F. Li, C. Zhang, Numerical and experimental investigations on the band-gap characteristics of metamaterial multi-span beams, Physics Letters A 383 (36) (2019) 126029. doi:https://doi.org/10.1016/j.physleta.2019.126029.

[19] H. Meng, D. Chronopoulos, A. Fabro, W. Elmadih, I. Maskery, Rainbow metamaterials for broadband multi-frequency vibration attenuation: Numerical analysis and experimental validation, Journal of Sound and Vibration 465 (2020) 115005. doi:https://doi.org/10.1016/j.jsv.2019.115005.
URL http://www.sciencedirect.com/science/article/pii/S0022460X19305681

[20] A. Carcaterra, A. Akay, C. Bernardini, Trapping of vibration energy into a set of resonators: Theory and application to aerospace structures, Mechanical Systems and Signal Processing 26 (2012) 1 – 14. doi:https://doi.org/10.1016/j.ymssp.2011.05.005.

[21] N. Roveri, A. Carcaterra, A. Akay, Energy equipartition and frequency distribution in complex attachments, The Journal of the Acoustical Society of America 126 (1) (2009) 122–128. doi:https://doi.org/10.1121/1.3147502.

[22] A. Carcaterra, A. Akay, I. Koc, Near-irreversibility in a conservative linear structure with singularity points in its modal density, The Journal of the Acoustical Society of America 119 (4) (2006) 2141–2149. doi:https://doi.org/10.1121/1.2179747.

[23] N. Hoang, P. Warnitchai, Design of multiple tuned mass dampers by using a numerical optimizer, Earthquake

Engineering & Structural Dynamics 34 (2) (2005) 125–144. doi:https://doi.org/10.1002/eqe.413.

[24] L. S. Vellar, S. P. Ontiveros-Pérez, L. F. F. Miguel, F. Miguel, L. Fleck, Robust optimum design of multiple tuned mass dampers for vibration control in buildings subjected to seismic excitation, Shock and Vibration 2019 (2019). doi:https://doi.org/10.1155/2019/9273714.

[25] A. Lucchini, R. Greco, G. C. Marano, G. Monti, Robust Design of Tuned Mass Damper Systems for Seismic Protection of Multistory Buildings, Journal of Structural Engineering 140 (8) (2014) A4014009. doi:https://doi.org/10.1061/(ASCE)ST.1943-541X.0000918.

[26] S.-Y. Kim, C.-H. Lee, Optimum design of linear multiple tuned mass dampers subjected to white-noise base acceleration considering practical configurations, Engineering Structures 171 (2018) 516–528. doi:https://doi.org/10.1002/stc.297.

[27] E. Dehghan-Niri, S. M. Zahrai, A. Mohtat, Effectiveness-robustness objectives in MTMD system design: An evolutionary optimal design methodology, Structural Control and Health Monitoring 17 (2) (2010) 218–236.

[28] C.-C. Lin, G.-L. Lin, K.-C. Chiu, Robust Design Strategy for Multiple Tuned Mass Dampers with Consideration of Frequency Bandwidth, International Journal of Structural Stability and Dynamics 17 (01) (2017) 1750002. doi:https://doi.org/10.1142/S021945541750002X.

[29] C. Sugino, Y. Xia, S. Leadenham, M. Ruzzene, A. Erturk, A general theory for bandgap estimation in locally resonant metastructures, Journal of Sound and Vibration 406 (2017) 104–123. doi:https://doi.org/10.1016/j.jsv.2017.06.004.

[30] L. Singleton, J. Cheer, S. Daley, Design of a resonator-based metamaterial for broadband control of transverse cable vibration (2019).

[31] S. Zouari, J. Brocail, J.-M. Génevaux, Flexural wave band gaps in metamaterial plates: A numerical and experimental study from infinite to finite models, Journal of Sound and Vibration 435 (2018) 246–263. doi:https://doi.org/10.1016/j.jsv.2018.07.030.

[32] D. Beli, A. T. Fabro, M. Ruzzene, J. R. F. Arruda, Wave attenuation and trapping in 3d printed cantilever-in-mass metamaterials with spatially correlated variability, Scientific reports 9 (1) (2019) 1–11. doi:https://doi.org/10.1038/s41598-019-41999-0.

[33] A. T. Fabro, H. Meng, D. Chronopoulos, Uncertainties in the attenuation performance of a multi-frequency metastructure from additive manufacturing, Mechanical Systems and Signal Processing 138 (2020) 106557. doi:https://doi.org/10.1016/j.ymssp.2019.106557.

[34] M. R. Souza, D. Beli, N. S. Ferguson, J. R. d. F. Arruda, A. T. Fabro, A bayesian approach for wavenumber identification of metamaterial beams possessing variability, Mechanical Systems and Signal Processing 135 (2020) 106437. doi:https://doi.org/10.1016/j.ymssp.2019.106437.

[35] W. Ma, J. Yu, Y. Yang, Graphical design methodology of multi-degrees-of-freedom tuned mass damper for suppressing multiple modes, Journal of Vibration and Acoustics 143 (1) (2021) 011008. doi:https://doi.org/10.1115/1.4047860.

[36] M. M. A. da Costa, D. A. Castello, C. Magluta, N. Roitman, On the optimal design and robustness of spatially distributed tuned mass dampers, Mechanical Systems and Signal Processing 150 (2021) 107289. doi:https://doi.org/10.1016/j.ymssp.2020.107289.

[37] Y. Ben-Haim, Info-gap decision theory: decisions under severe uncertainty, 2nd Edition, Elsevier/Academic Press, Amsterdam, 2006.

[38] K. L. V. Buren, S. Atamturktur, F. M. Hemez, Model selection through robustness and fidelity criteria: Modeling the dynamics of the CX-100 wind turbine blade, Mechanical Systems and Signal Processing 43 (1) (2014) 246 – 259. doi:https://doi.org/10.1016/j.ymssp.2013.10.010.
URL http://www.sciencedirect.com/science/article/pii/S088832701300513X

[39] Robust assessment of collapse resistance of structures under uncertain loads based on Info-Gap model 285 (2015) 208 – 227. doi:https://doi.org/10.1016/j.cma.2014.10.038.

[40] K. Jaboviste, E. Sadoulet-Reboul, N. Peyret, C. Arnould, E. Collard, G. Chevallier, On the compromise between performance and robustness for viscoelastic damped structures, Mechanical Systems and Signal Processing 119 (2019) 65–80. doi:https://doi.org/10.1016/j.ymssp.2018.08.061.
URL https://www.sciencedirect.com/science/article/pii/S0888327018306071

[41] C. Sugino, S. Leadenham, M. Ruzzene, A. Erturk, On the mechanism of bandgap formation in locally resonant finite elastic metamaterials, Journal of Applied Physics 120 (13) (2016) 134501. doi:https://doi.org/10.1063/1.4963648.

[42] G. Raze, G. Kerschen, H∞ optimization of multiple tuned mass dampers for multimodal vibration control, Computers & Structures 248 (2021) 106485. doi:https://doi.org/10.1016/j.compstruc.2021.106485.
URL https://www.sciencedirect.com/science/article/pii/S0045794921000079

[43] E. Balmes, Sensors, degrees of freedom, and generalized modeshape expansion methods,# 8, in: Proceedinges - SPIE The International Society for Optical Engineering, Vol. 3727, SPIE INTERNATIONAL SOCIETY FOR OPTICAL, 1999, pp. 628–634.

Appendix A. Parameters

Tab.A.3 contains the geometrical and material parameters used for the numerical simulations.

Parameter	Variable [Unit]	Value
Geometrical Parameters		
Parameters for the fuselage		
L_f	Length [m]	0.46
d_f	outer diameter [m]	0.05
h_f	thickness [m]	0.002
Parameters for the wings		
L_w	length [m]	0.6
h_w	thickness [m]	0.001
Parameters for the stabilizers		
L_{vs}	length [m]	0.07
w_{vs}	base width [m]	0.04
h_{ws}	thickness [m]	0.00145
Parameters for the Horizontal Stabilizer		
Materials for the airplane		
1 - Wing and stabilizers		
E_1	Young's modulus [GPa]	192
ρ_1	density [kg.m^{-3}]	7721
ν_1	Loss factor [%]	0.113
2 - Angle bars		
E_2	Young's modulus [GPa]	70
ρ_2	density [kg.m^{-3}]	2694
ν_2	Loss factor [%]	0.28
3 - Fuselage		
E_3	Young's modulus [GPa]	70
ρ_3	density [kg.m^{-3}]	2775
ν_3	Loss factor [%]	0.28
4 - Interface wing/angle bar		
E_4	Young's modulus [GPa]	13.3614
ρ_4	density [kg.m^{-3}]	2694
ν_4	Loss factor [%]	0.235218
5 - Interface stabilizers/angle bar		
E_5	Young's modulus [GPa]	16.0891
ρ_5	density [kg.m^{-3}]	2694
ν_5	Loss factor [%]	0.112735
Material for the absorbers		
E_{abs}	Young's modulus [GPa]	4.1
ρ_{abs}	density [kg.m^{-3}]	1156.5
η_{abs}	Loss factor [%]	6.6

Table A.3: Parameters used for the numerical simulations

Highlights

- The performance and robustness of different metabsorber configurations are compared.
- Numerical studies rely on the FEM method and energy quantities.
- Robustness is estimated with the Info-Gap method considering lack-of-knowledge.
- Numerical results are compared to experimental measurements for an airplane model.

Declaration of interests

☐ The authors declare that they have no known competing financial interests or personal relationships that could have appeared to influence the work reported in this paper.

☒ The authors declare the following financial interests/personal relationships which may be considered as potential competing interests:

Emeline Sadoulet-Reboul has patent #WO2020165128 issued to THALES SA, CNRS, UFC.

Highlights

- The performance and robustness of different metabsorber configurations are compared.
- Numerical studies rely on the FEM method and energy quantities.
- Robustness is estimated with the Info-Gap method considering lack-of-knowledge.
- Numerical results are compared to experimental measurements for an airplane model.